IEEE Access
Multidisciplinary | Rapid Review | Open Access Journal

IEEE MAGNETICS SOCIETY SECTION

Received 25 April 2024, accepted 19 May 2024, date of publication 27 May 2024, date of current version 18 June 2024.

Digital Object Identifier 10.1109/ACCESS.2024.3405980

APPLIED RESEARCH

Investigation and Implementation of Miniaturized Microwave System for Linear Array Antenna Loaded With Omega Structures Planar Array

AHMED F. MILIGY[1], FATMA TAHER[2], (Senior Member, IEEE), MOHAMED FATHY ABO SREE[3], SARA YEHIA ABDEL FATAH[4,5], THAMER ALGHAMDI[6], AND MOATH ALATHBAH[7]

[1]Air Defence College, Alexandria University, Alexandria 18711, Egypt
[2]College of Technological Innovation, Zayed University, Dubai, United Arab Emirates
[3]Department of Electronics and Communications Engineering, Arab Academy for Science, Technology and Maritime Transport, Cairo 11799, Egypt
[4]Department of Mechatronics Engineering and Automation, Faculty of Engineering, Egyptian Chinese University, Cairo 19346, Egypt
[5]Higher Institute of Engineering and Technology, El-Tagmoe El-Khames, New Cairo 11765, Egypt
[6]Wolfson Centre for Magnetics, School of Engineering, Cardiff University, CF10 3AT Cardiff, U.K.
[7]Department of Electrical Engineering, College of Engineering, King Saud University, Riyadh 11451, Saudi Arabia

Corresponding author: Thamer Alghamdi (alghamdit1@cardiff.ac.uk)

This work was supported by King Saud University, Riyadh, Saudi Arabia, through the Researchers Supporting Project under Grant RSPD2024R868.

ABSTRACT This paper investigates and implements a miniaturized microwave system for microstrip linear array antenna that operates in X-band (10.1 GHz), S-band (3.4 GHz) and C-band (5.6 GHz). The microwave system consists of three parts: a power divider, a directional coupler, and a matching network stub. These systems feed a linear array (16 elements) of patch antennas loaded with resonance planar omega structures array (160 elements) distributed in both patch (64 elements) and ground (96 elements) as the metamaterial structures for miniaturization purpose. The 1-to-2 divider feeds two directional couplers that act as phase shifters. The couplers fed a set of 1-to-4 dividers that in return feed a series of patch antennas. The system has been simulated and measured using microwave analyzer. The system is designed, analyzed and implemented using Roger substrate of thickness 1.27mm and 10.2 dielectric constant and simulated using HFSS. The proposed miniaturized array introduces a gain of 8, return loss of -24 dB and radiation efficiency of 90%. There is a good agreement between the simulation results and the measured values. The proposed array covers applications in mobile communication systems and Wi-MAX.

INDEX TERMS Miniaturized antenna, array antenna, resonant structures, omega structures, divider, coupler.

I. INTRODUCTION

Multiple technologies have been devised to make types of antennas for mobile communication systems, Wi-MAX and other microwave applications. It is quite a challenge to achieve multiband operation over a wide bandwidth with a compact antenna design. Microstrip technologies are, easy and less expensive compared with waveguide technologies, but have the disadvantages of radiation loss and not being shielded thus; introducing a compact dual resonating microstrip array antenna that covers a wide bandwidth is a good candidate for microwave applications. The compact size of the array makes it suitable for use in the mobile base stations and wireless routers to serve mobile consumers in long hallways, corridors, and tunnels [1], [2], [3]. Over the past few years, there has been a sharp rise in demand

The associate editor coordinating the review of this manuscript and approving it for publication was Philip Pong.

for inexpensive, small, and compact antennas. Applications for various microstrips patch antenna types are covered. This paper proposes a compacting approach using resonance circuit structures and metamaterial due to the need for smaller antennas in both military and commercial applications [4], [5], [6]. A class of ordered composite materials known as metamaterials possesses remarkable qualities that are severely to find in the natural world. Another technology involves the use of metamaterial antennas. A combination of the metamaterial and micro-patch antenna is used to improve the performance of the ordinary patch antenna. Metamaterial structures are also known as resonance structures because it changes the resonating frequency with the need to change the dimensions [7], [8], [9]. The properties result from the addition of artificially created, extrinsic, low dimensional inhomogeneities, which give rise to qualitatively new response functions not found in the constituent materials. These materials are referred to as double negative (DNG) materials because they have both negative permittivity and permeability. Because they adhere to the left-hand rule, they also have a negative refractive index (NRI), which is why they are also referred to as left-handed materials or NRI materials. They provide some intriguing modifications to an antenna's radiation characteristics due to their peculiar qualities [8], [9], [10]. Because of the rapid advancements in subwavelength imaging and nanofabrication, the concept of MTMs has gained traction in research. Hybrids are helpful in the design of electronically variable attenuators, microwave mixers, modulators, dividers, couplers and many other microwave systems and components because of the 90° phase difference between the outputs. In this paper, an investigation of a miniaturized set of microwave systems designed to feed an array of microstrip linear antennas is made. This novel design integrates all the microwave systems while maintaining matching. The miniature size and dimensions are noteworthy as the antenna array operates in the X-band, S-band and C-band without the need to reconfigure or sacrifice the size, all thanks to the introduction of the omega resonance structures. The Microwave system consists of four parts: a power divider, a directional coupler, a matching network stub, linear patch antenna loaded with a planar array of omega structures. The 1-to-2 divider feeds two directional couplers that act as phase shifters. The Couplers fed a set of 1-to-4 dividers that in return feed a series of patch antennas. The proposed system is based on the concept of a microstrip linear array antenna loaded with an array of omega structures. The Paper is organized as follows. Section II introduces and analyzes the design and results of each microwave elements include: the Wilkinson divider, the directional coupler, and the matching circuits. In Section III, the design and analysis of resonance omega structures array. Section IV introduces the patch antenna array loaded with the omega structure array for miniaturization. The miniaturized array simulated and measured results is presented and compared in section V. Section VI makes a comparison with other related works, and finally concludes and reports the research work.

II. MICROSTRIP ELEMENTS ANALYSIS AND DESIGN

This Higher operating frequency integrated circuits are needed for space applications, electronic warfare, radars, and communication systems. Utilizing the millimeter wave region of the spectrum allows for smaller products, more efficient use of the spectrum, and higher data rates. In these kinds of applications, power dividers, couplers and stubs serve as basic components that split and combine radio frequency signals. This section introduce the design methodology and simulation results for the proposed elements using Eqns. (1), (2) and (3) [11] to determine the width and length of transmission lines which construct these elements for 50 ohm characteristic impedance using Rogger substrate of 10.2 dielectric constant and 1.27 mm thickness.

$$\frac{W}{h}=\begin{cases}\dfrac{8e^{A}}{e^{2A}-2} & \text{for } \dfrac{W}{h}<2\\ \dfrac{2}{\pi}\left[B-1-\ln(2B-1)+\dfrac{\varepsilon_r-1}{2\varepsilon_r}\left(\ln(B-1)+0.39-\dfrac{0.61}{\varepsilon_r}\right)\right] & \text{for } \dfrac{W}{h}>2\end{cases} \tag{1}$$

$$A=\frac{Z_0}{60}\sqrt{\frac{\varepsilon_r+1}{2}}+\frac{\varepsilon_r-1}{\varepsilon_r+1}\left(0.23+\frac{0.11}{\varepsilon_r}\right) \quad \text{and}$$

$$B=\frac{377\pi}{2Z_0\sqrt{\varepsilon_r}} \tag{2}$$

$$\varepsilon_e=\frac{\varepsilon_r+1}{2}+\frac{\varepsilon_r-1}{2}\frac{1}{\sqrt{1+12h_R/w_{T1}}} \quad \text{and } \lambda_g$$

$$=\left(3\times10^{8}/f\sqrt{\varepsilon_e}\right) \tag{3}$$

A. THE −3 dB WILKINSON POWER DIVIDER STRUCTURE

Power dividers are considered one of the microwave circuit components which are used in different applications such multiplexers, couplers and antenna systems. The power dividers are used to equally split signal power in a system. The low loss capacity and high-quality factor can be obtained using rectangular waveguide power divider for microwave applications but the high cost and volume are drawbacks of this technology. Microstrip technologies overcome the drawback of cost and volume, but still have a disadvantage of high radiation loss which limits using these technologies in different applications. There are several types as dividers: T, Y and Wilkinson power divider. Among the most popular topologies is the Wilkinson power divider, which offers low insertion loss and high return loss isolation. Wilkinson power dividers are fundamental components used in various applications, including phased arrays and linear arrays [11]. Wilkinson dividers offer numerous benefits, including a straightforward design, compact dimensions, low loss, high isolation between ports, wide bandwidth, matched output ports, and minimal insertion loss. This section proposes a Wilkinson microstrip power divider, which is the basic one that will be used to construct a four-output port divider as shown in Fig.1 with the main dimensions for the proposed divider using Eqns. (1), (2) and (3). In this design, Wilkinson dividers were used as it achieves low loss and has high levels of isolation between

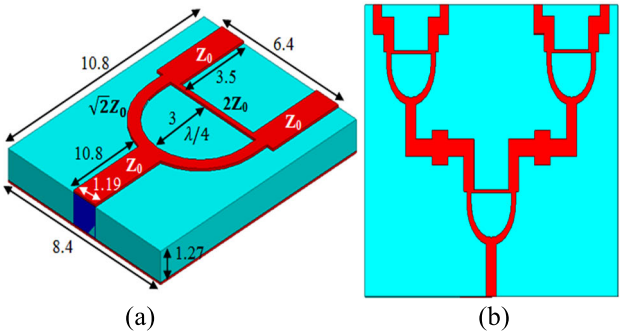

FIGURE 1. The main dimensions [mm] of the wilkinson power divider: (a) The two output ports divider. (b) The four output ports divider.

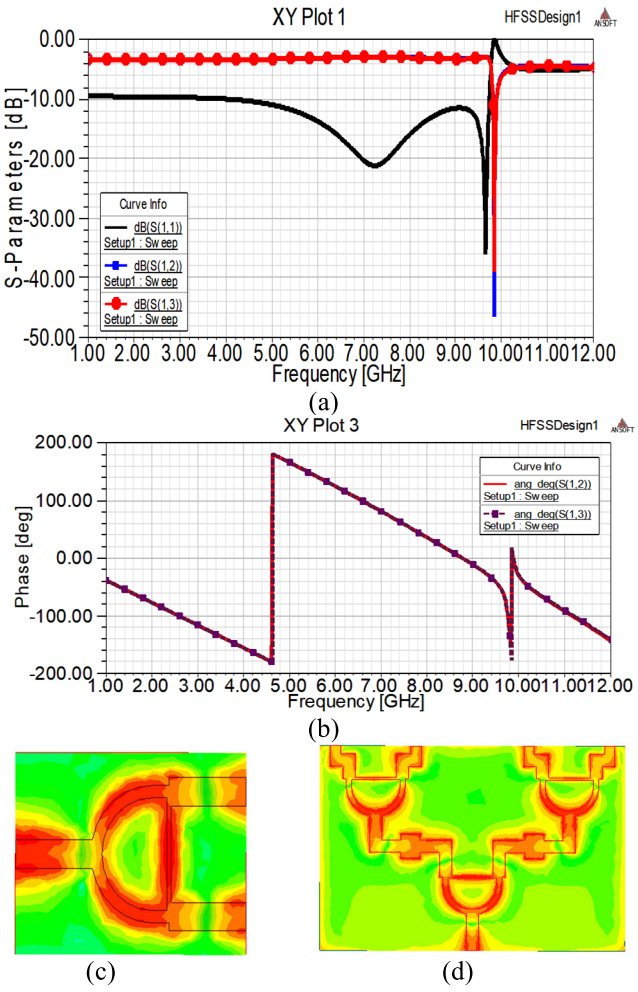

FIGURE 2. Wilkinson power divider simulation results. (a) The S-Parameters [dB]. (b) The phase shift [deg.]. (c) The 2-O/P ports E-Field distribution [V/m]. (d) The 4-O/P E-Field distribution [V/m].

ports. First, a two-port power divider is implemented to feed a directional coupler. The output of the coupler feeds 2 two port dividers which in return feed a 4-port divider. The output of the 4-port dividers is the input of each of the 16 patch elements in the linear array.

Simulation results for the proposed Wilkinson divider, in which input power at port 1 is transmitted equally (−3 dB) to two isolated output ports 2 and 3 and in-phase are shown in Fig.2 with the electric field distribution over structures.

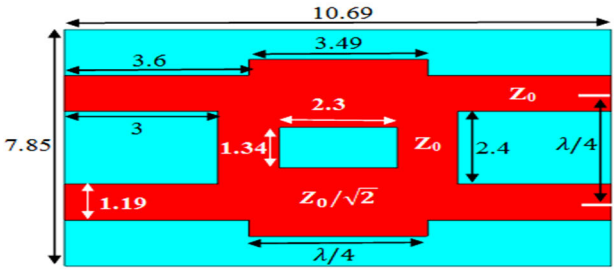

FIGURE 3. Main dimensions [mm] of the microstrip directional coupler.

B. THE MICROSTRIP DIRECTIONAL COUPLER STRUCTURE

A directional coupler is being implemented to act as a phase shifter as seen in Fig.3. The ports of the coupler are matched load. The output of the coupler is a halved (− 3 dB) signal in each of the two branches and both signals are out of phase. The −3dB coupler meets specifications for operational bandwidth, frequencies, and size while offering equal and out-of-phase transmission power. In communication systems, a broadband coupler is used to separate the receiver port from the transmitters [11]. The directional coupler in this section, divides input power equally at output ports with a 90-degree phase shift for antenna applications, and is presented with an equal coupling coefficient and insertion loss. Its main dimensions are illustrated in Fig.3.

Simulation results such as transmission coefficient, phase shift and the electric field distribution for the proposed coupler, in which input power at port 1 is transmitted equally (−3 dB) to two isolated output ports 2 and 3 and out-phase are shown in Fig.4. At 10 GHz with a −3 dB coupling, Figure 4(a) depicts the intersection of the S11 curves for ports 2 and 3, indicating equal reflection from both ports. This convergence implies that incoming signals experience an identical level of reflection at ports 2 and 3, resulting in an equitable division of power between them. In practical terms, if 1 unit of power enters the coupler through port 1, approximately 0.5 units of power will emerge from each of ports 2 and 3. This balanced power division is a hallmark characteristic of a 3 dB directional coupler, pivotal for applications like power monitoring and signal distribution, where maintaining equal power levels across branches is essential for system performance. Meanwhile, Figure 4(b) delves into the phase relationship between ports 2 and 3, revealing a 90-degree phase difference at 10 GHz. This phase offset is a direct consequence of the coupler's internal design and the electromagnetic coupling mechanism between its microstrip lines. While this phase difference is consistent at 10 GHz, it's important to acknowledge that it may vary with frequency and specific design parameters of the coupler. Nonetheless, understanding this phase discrepancy is fundamental, especially in applications requiring precise phase control or coherence preservation, such as phased array antennas or

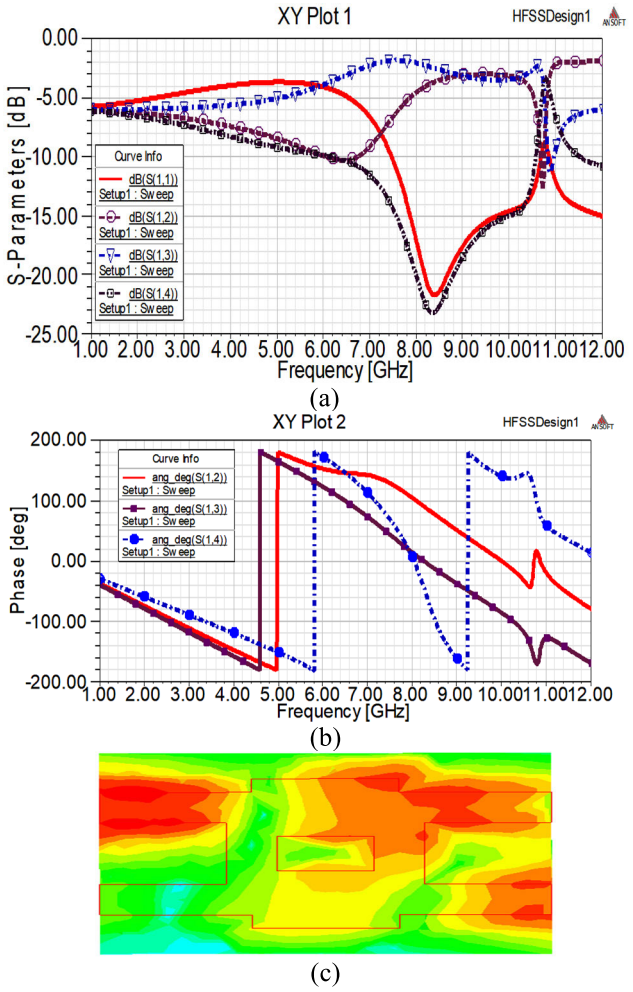

FIGURE 4. Microstrip directional coupler simulation results. (a) The S-Parameters [dB]. (b) The phase shift [deg.]. (c) The E-Field [V/m].

coherent communication systems. Lastly, Figure 4(c) offers insight into the E-field distribution within the directional coupler. Here, the even distribution of the E-field between ports 2 and 3 confirms the equal division of power between these ports. Additionally, the isolation observed at port 4 signifies minimal power coupling to this port, making it suitable for applications where signal monitoring or extraction is unnecessary. Conversely, port 1 serves as the primary input port, where signals are introduced to the coupler for further processing or distribution. Collectively, these details provide a comprehensive understanding of the behaviour of the 3 dB directional coupler at 10 GHz. They highlight the intricate interplay between power division, phase relationships, and the functional roles of each port within the coupler, essential considerations for designing and integrating such couplers into complex microwave and RF systems.

C. THE MATCHING NETWORK STUBS

In microwave and radio-frequency engineering, a stub, also known as a resonant stub, refers to a segment of transmission

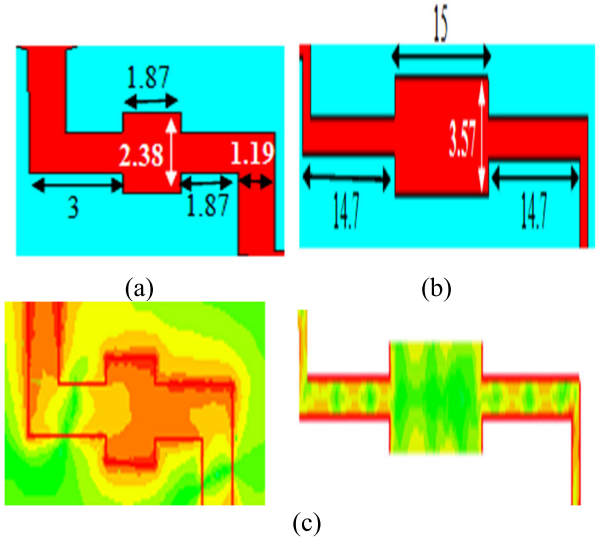

FIGURE 5. Matching network stub dimensions and simulation results. (a) The dimensions [mm]. (b) The electric field distribution [V/m].

line or waveguide connected at one end only, with the other end either open-circuited or short-circuited. The input impedance of the stub, disregarding transmission line losses, is purely reactive—either capacitive or inductive—depending on its electrical length and termination. Stubs serve various functions such as capacitors, inductors, and resonant circuits at radio frequencies, primarily attributed to standing waves along their length, with their reactive characteristics determined by their physical dimensions relative to the wavelength of the radio waves. Particularly in microwave circuits where wavelengths are relatively short, stubs find extensive application, often replacing discrete capacitors and inductors due to the poor performance of lumped components at microwave frequencies owing to parasitic reactance. Commonly utilized in antenna impedance matching, frequency selective filters, and resonant circuits for UHF electronic oscillators and RF amplifiers, stubs can be fashioned from various transmission line types including parallel conductor lines (known as Lecher lines), coaxial cables, straplines, waveguides, and dielectric waveguides. Designing stub circuits can be facilitated by employing a Smith chart, a graphical aid for determining the appropriate line length to achieve a desired reactance. Simple matching circuits are necessary to maintain the matching between the different microwave systems. matching circuits are placed between the two-port power divider stage and the directional coupler stage, as well as between the directional coupler and the 4-port dividers stage. Fig.5 (a) shows the design and of the matching network stub between both stages respectively. Fig.5 (b) shows the electric field distribution of the matching networks. Matching between microwave sections is an essential part for required system performance. The required impedance matching for the proposed microwave elements connection has been obtained using matching network stub for 50 ohm impedance matching [11].

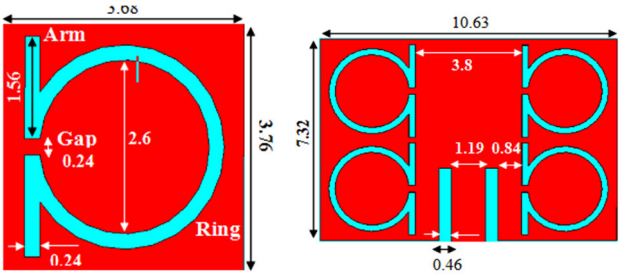

FIGURE 6. The omega structure dimensions [mm]. (a) The unit cell. (b) The array.

III. RESONANT OMEGA PLANAR ARRAY STRUCTURE

Resonance omega structures are classified as metamaterial structures. Metamaterials are a new class of ordered composites that exhibit exceptional properties not readily observed in nature. These properties arise from qualitatively new response functions that are not observed in the constituent materials and result from the inclusion of artificially fabricated, extrinsic, low dimensional inhomogeneities. Such material exhibits permittivity and permeability both negative, and hence they are known as the double negative (DNG) materials. And so they have Negative Refractive Index (NRI), and hence they are also called as the Negative Refractive Index materials or Left-handed material LHM (as they follow left-hand rule). Because of their unusual properties, they offer some interesting changes in radiation characteristics of an antenna. The idea of MTMs has been quickly adopted in research, due to rapidly developing nanofabrication and subwavelength imaging techniques [7], [8], [9], [10], [11], [12], [13], [14]. It has recently been discovered that a wide range of metallic and semiconductor resonant circuits and metamaterials exhibit complete absorption of electromagnetic radiation. A wide range of frequencies, including the microwave, THz, and visible regions, have all seen reports of this effect. Numerous varied applications have already been put forth. Radar, photovoltaics, electromagnetic compatibility, biosensing, thermal source emission, and thermal bolometer are a few of them [12], [13], [14]. Even though the structures that exhibit total absorption may vary greatly from one another, they all share the following traits: total absorption can only be reached under certain conditions imposed on the material's properties or the structure's geometry; energy transmission through the structure is prohibited; and the structure has an intrinsic resonance. A planar resonance or metamaterial with an absorptive layer separating it from the ground plane and a lattice of metallic patches is one of the metamaterial structures that has been extensively discussed in the literature with regard to highly efficient absorbers. When the electromagnetic radiation is trapped beneath the patch, a structure with a thickness of less than a wavelength can demonstrate the effect of total absorption. Numerous. This section presents a basic physical model that describes the properties of a resonance omega planar array structure shown in Fig.6 with its main dimensions for both unit cell and array.

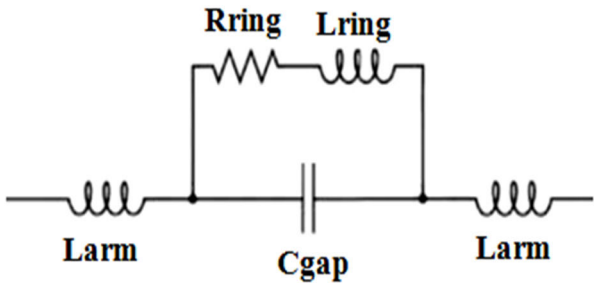

FIGURE 7. The omega structure unit cell equivalent circuit.

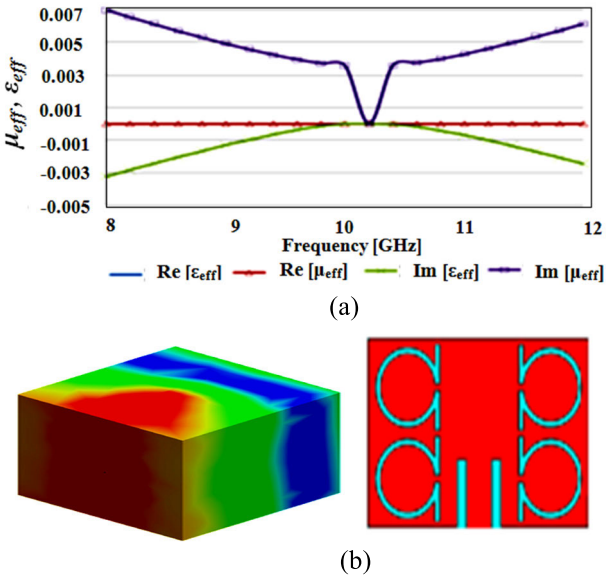

FIGURE 8. The omega structure simulation results.(a) real and imaginary parts of [e_eff and μ_eff]. (b) E-Field Distribution [V/m].

We use the RLC circuit model to give a broad overview of the impact of total absorption independent of the specific geometry of the patch. A structured surface is regarded as load impedance at the transmission line's end in the RLC model, which models the free space. First; let's discuss the Meta surface's effective surface impedance, or Zeff. In this instance, the Meta surface reflection can be characterized uniformly, regardless of the structuring type. We characterize, in terms of its equivalent resonant RLC, the resonance of the TM mode excited by a normally incident plane wave and squeezed between the patch and ground plane [7], [8], [9]. The corresponding RLC circuit for the proposed omega structure for the TM mode for the resonant circuit of Fig.6 is shown in Fig.7. The main physical characteristics of the resonant structures are described by this circuit, which also includes [12], [13], [14]: the total resistance R, which controls the power absorbed because of ohmic losses; the total inductance L, which is produced by the finite electric currents oscillating in the ground plane and metallic patch; the total capacitance C, which describes the charge accumulation brought on by the external field.

The structure under consideration, is shown in Fig.6 is a periodic arrangement of 160 elements omega structure planar

array distributed in both patch and ground and spaced s ≪ λ (where λ is the wavelength) above a ground plane. We include an absorptive layer with a weak loss tangent between the patch and the ground plane. The structure absorbs electromagnetic energy poorly. Nonetheless, the entire absorption effect would be attained if the free-space impedance (purely resistive), Z0 = 120π Ω, were matched to the surface's impedance. This would cause the incident energy to be entirely converted into Ohmic losses inside the absorptive layer. Inversely proportional to the layer thickness, the electronic resistance R of the absorptive layer is incredibly large in relation to the free-space impedance Z0 if we assume that the electric current induced in the layer by an incident plane wave oscillates along the patch side. An intrinsic resonance may be used to solve the impedance matching problem. At the resonance, the effective electric resistance, or real part of the effective impedance, can be significantly reduced as shown in Fig.8

In this section, omega structures have been designed and analyzed. The real and imaginary parts of the permittivity and permeability have been obtained based on the scattering parameters in a waveguide. The proposed omega structures, the index of refraction n ≈ 0 would occur at the frequencies where ε eff and/or μ eff ≈ 0. Ideally, the proposed omega structures were optimized to obtain the desired properties at the operating frequency band as shown in Fig.8

IV. MICROSTRIP LINEAR ARRAY ANTENNA LOADED WITH PLANAR ARRAY OF OMEGA STRUCTURES

Proposed patch antenna is a design using artificial substrate made up of metamaterial using omega structure. Here omega structures are used to make metamaterial design. When omega structures loaded antenna, then they simultaneously offer negative permittivity and negative permeability and hence it becomes double negative metamaterial. The resonance frequency of the proposed antenna will shifted down to a lower frequency and this is the required miniaturization as antenna operates in lower frequency with small and compact dimensions using metamaterials. Proposed patch antenna is a design using artificial substrate made up of metamaterial using omega structure. Here omega structures are used to make metamaterial design. When omega structures loaded antenna, then they simultaneously offer negative permittivity and negative permeability and hence it becomes double negative metamaterial. The resonance frequency of the proposed antenna will shift down to a lower frequency and this is the required miniaturization as antenna operates in lower frequency with small and compact dimensions using metamaterials. Currently in demand due to their advantages and ability to satisfy the need for small, lightweight antennas that are compatible and simple to integrate, microstrip antennas are widely used. In this section a rectangular patch is designed as a reference element using Rogger substrate of 10.2 dielectric constant for X-band applications using Eqns. (4), (5) and (6) [15], [16], [17], [18], [19], [20] and then loaded with the omega structure planar array. The omega array consists

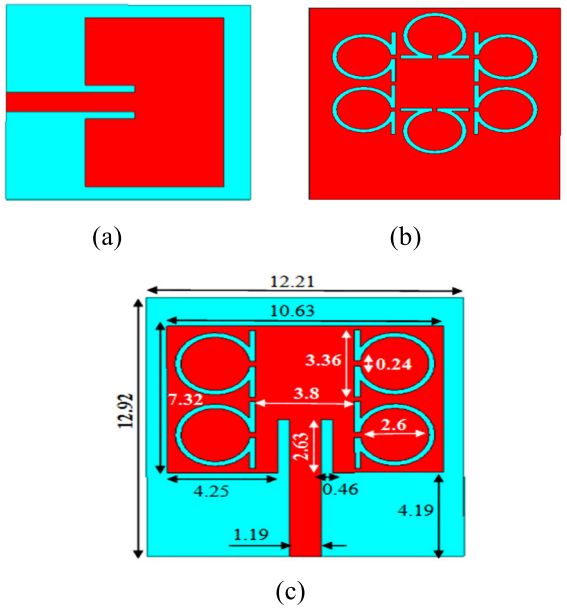

FIGURE 9. The antenna dimensions [mm]. (a) The element without omega. (b) The back view of element loaded with omega. (c) The top view of element loaded with omega.

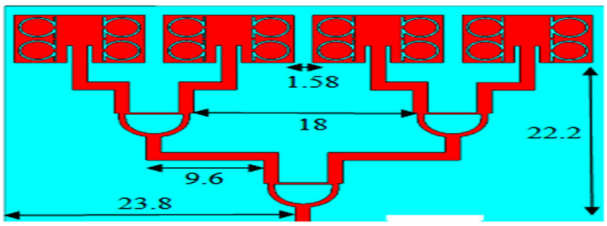

FIGURE 10. The 1 × 4 Linear array loaded with omega structures.

of four elements on patch and 6 elements on ground with dimensions as shown in Fig.9 (a, b and c).

$$W_r = \frac{1}{2f_r\sqrt{\mu_0\varepsilon_0}}\sqrt{\frac{2}{\varepsilon_r+1}} = \frac{v_0}{2f_r}\sqrt{\frac{2}{\varepsilon_r+1}} \tag{4}$$

$$\frac{\Delta L}{d} = 0.412\frac{(\varepsilon_{reff}+0.3)\left(\frac{W}{d}+0.264\right)}{(\varepsilon_{reff}-0.258)\left(\frac{W}{d}+0.8\right)} \tag{5}$$

$$L_r = \frac{1}{2f_r\sqrt{\varepsilon}_{reff}\sqrt{\mu_0\varepsilon_0}} - 2\Delta L = \frac{\lambda}{2} - 2\Delta L \tag{6}$$

Four elements 1 × 4 linear array patch antenna loaded with omega structure planar array is constructer using three dividers as shown in Fig.10. Copper is used for the patch materials and Rogger is used for the substrate material. By sweeping the parameters to achieve the required return loss, VSWR, gain, bandwidth, and directivity, the value of the initial antenna parameters will be optimized.

The 1 × 2 and 1 × 4 array's rectangular microstrip antenna loaded with omega structures design compared with the reference patch without omega structures has been optimized and the simulation results such as return loss, surface current, gain and the radiation pattern comparison simulation results are shown in Fig.11.

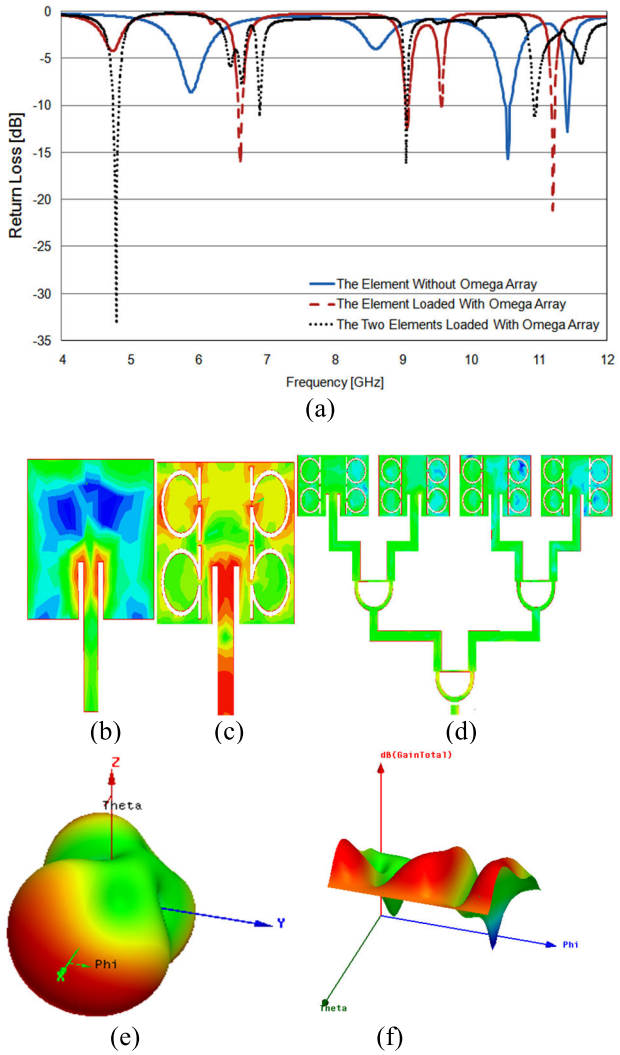

FIGURE 11. The antenna simulation results. (a) The return loss [dB] (b) The element without omega Js [A/m]. (c) The element with omega Js [A/m]. (d) The array with omega Js [A/m]. (e) The array 3D polar radiation pattern [dB]. (f) The array antenna gain [dB].

TABLE 1. Element and array without/with omega structures.

	Element Without Omega		Element Loaded With Planar Omega Array Structures				Two Elements Loaded With Planar Omega Array Structures			
f [GHz]	10.6	11.6	6.6	9.2	9.6	11.3	4.9	6.9	9.2	11
RL [dB]	-15	-13	-15	-13	-10	-20	-33	-11	-16	-11

The suggested linear array antennas loaded with the planar omega array are compared.Fig.11 (a) displays the return loss characteristics for the suggested antenna as well as the conventional antenna. Table 1 introduces the return loss in dB for the element and two elements antennas without and with omega structure array. The suggested metamaterial-based

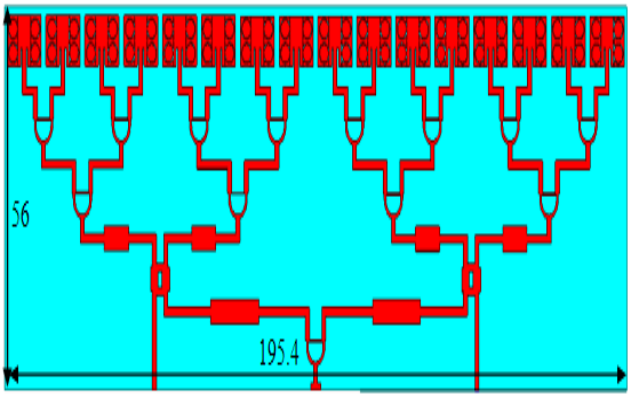

FIGURE 12. The full proposed miniaturized antenna array system.

TABLE 2. Miniaturized antenna array system loaded with omega planar array return loss [dB] for S,C and X-bands.

	S-Band			X-Band			
f[GHz]	2.3	2.8	3.4	8	9.2	10.1	11.5
RL[dB]	-9	-6	-22	-12	-10	-24	-10
	C-Band						
f[GHz]	4.2	4.5	5.6	5.8	6.5	6.9	7
RL[dB]	-14	-10	-18	-17	-10	-15	-17

antenna is tuned to respond similarly to a conventional patch antenna. After careful examination, it is discovered that, in comparison to the traditional simple rectangular patch antenna, the suggested metamaterial-based antenna requires less space. The proposed array which designed in X-band now operate in both C and S-bands using omega structure array. Thus, the metamaterial idea has been successfully applied to antenna miniaturization. In Figure 11, a comparative analysis is conducted among three antenna configurations: a single-element patch, a single-element patch loaded with an omega array, and a two-element patch loaded with an omega structure. Firstly, in Figure 11(a), the return loss characteristics are investigated. The single patch antenna operates efficiently at 10 GHz with a return loss of −15 dB. Upon loading the single patch with an omega structure, the antenna's operational frequency range shifts to the lower range of 6-7 GHz while maintaining the same −15 dB return loss. Remarkably, the two-element patch loaded with an omega structure achieves an impressive return loss of −35 dB at frequencies below 5 GHz. This significant improvement suggests the effectiveness of the omega structure in enhancing the antenna's performance, enabling miniaturization without compromising performance at lower frequencies. Next, Figures 11(b), (c), and (d) delve into the current distribution within the antennas. The absence of blue or red circles, indicative of efficient current distribution, is observed more prominently in the two-element omega-loaded configuration compared to the single-element configurations. This efficiency enhancement is attributed to the frequency ruler mechanism, underscoring the advantages

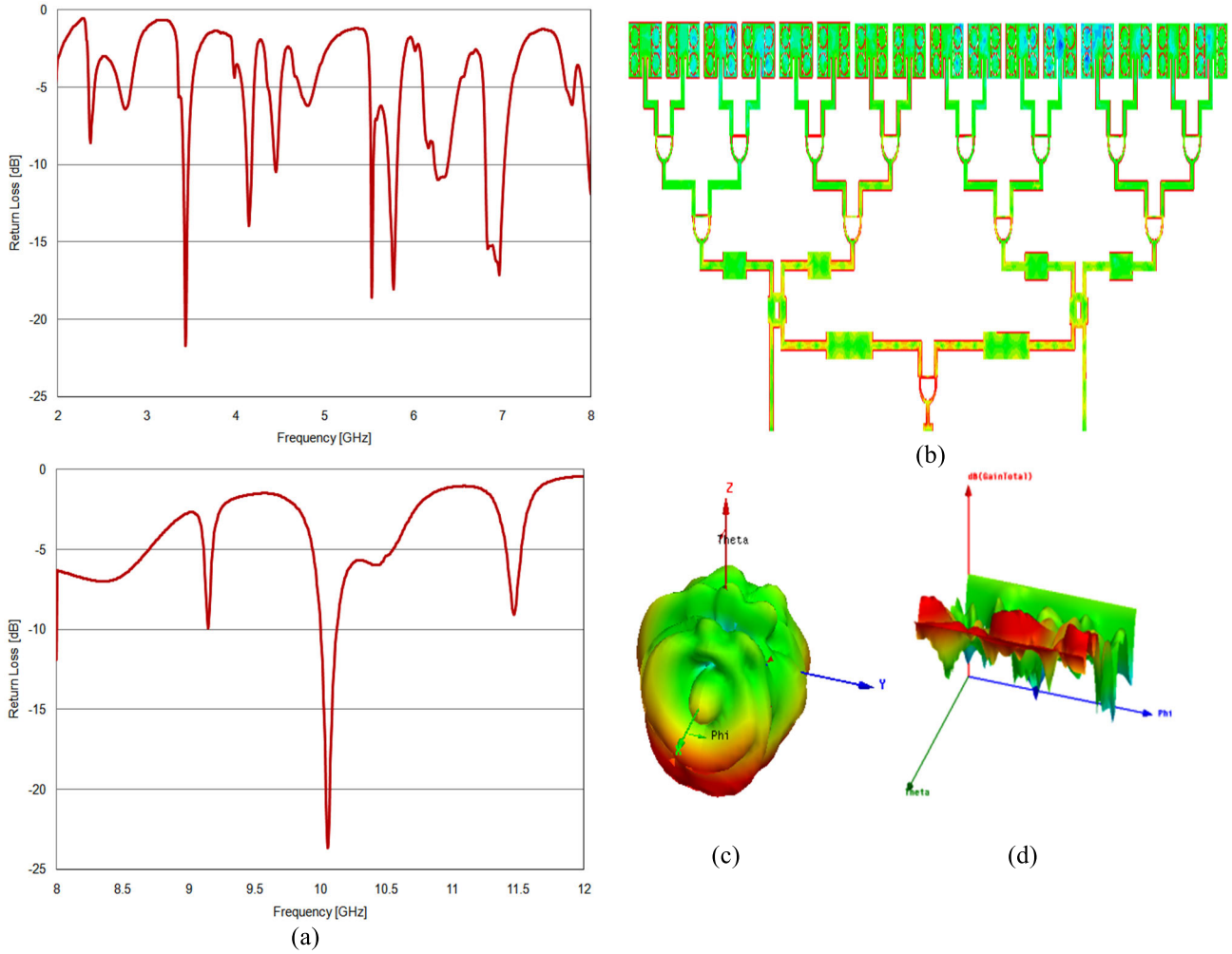

FIGURE 13. The full system simulation results. (a) The return loss [dB] (b) The system Js [A/m]. (c) The system 3D polar radiation pattern [dB]. (d) The array antenna gain [dB].

of utilizing multi-element configurations with omega structures. Furthermore, Figures 11(e) and (f) illustrate the 3-D radiation patterns for the single-element and two-element antennas with omega structures. These patterns demonstrate high gain, particularly noticeable in the two-element configuration with the omega structure, indicating superior radiation performance. Finally, Table 1 summarizes the key findings, providing a comprehensive overview of the antenna configurations' performance across various parameters, including operating frequency, return loss, current distribution efficiency, and radiation pattern characteristics. These detailed analyses underscore the significance of employing omega structures and multi-element configurations in optimizing antenna performance for diverse applications.

V. MINIATURIZED ANTENNA ARRAY SYSTEM

Currently in demand due to their advantages and ability to satisfy the need for small, lightweight antennas that are compatible and simple to integrate, microstrip antennas are widely used [21], [22], [23], [24], [25], [26]. With the help of this study, a rectangular patch microstrip antenna with 16 elements loaded with 160 elements of omega structure planar array distributed in both patch (64 elements) and ground (96 elements) and then integrated with 13 dividers and two directional coupler as shown in Fig.12.

A. THE FULL SYSTEM SIMULATION RESULTS

By sweeping the parameters to achieve the required return loss, VSWR, gain, bandwidth, current distribution and directivity, the value of the initial antenna parameters will be optimized. The full system simulation results shown in Fig.13 and the operating frequencies in S, C and X-Bands are tabulated in table 2.

B. THE FULL SYSTEM IMPLEMENTATION AND MEASURED RESULTS

Photographs of the proposed system at the microwave laboratory and comparison results are shown in Fig. 14. The implemented system is shown in Fig. 14(a) and the measured results are shown in Fig. 14(b). The Comparison between simulated and measured results are shown in Fig.14(c) with

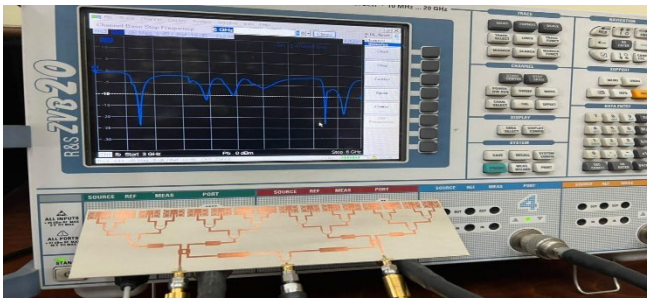
(a)

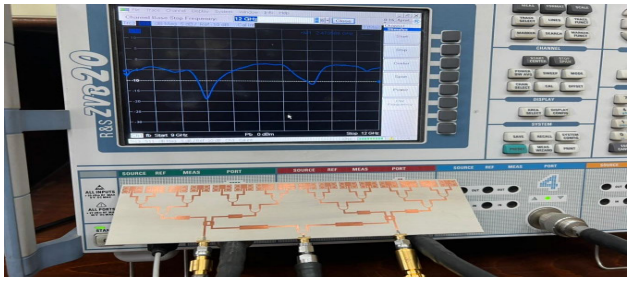
(b)

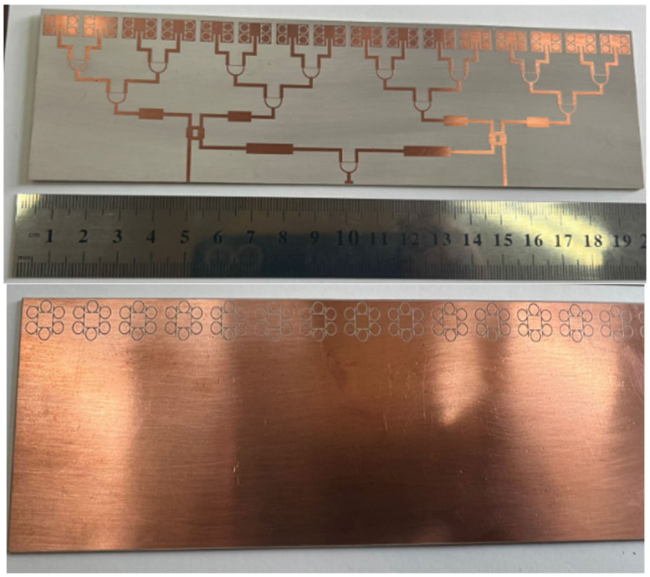
(c)

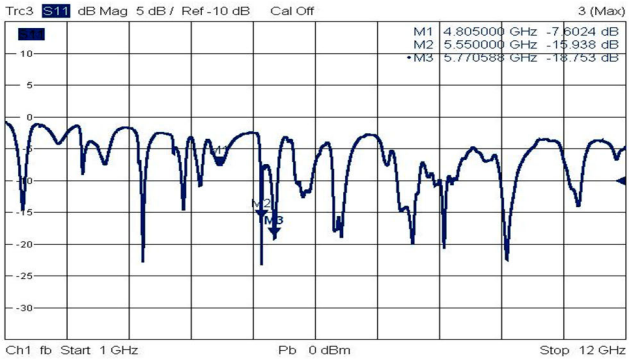

(d)

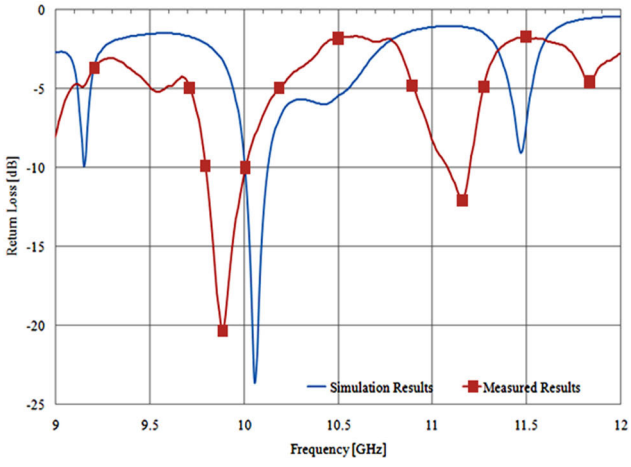

(e)

FIGURE 14. The full system implementation and comparison results (a), (b) and (c) The implemented system (d) The return loss measurement [dB]. (e) The comparison between simulated and measured results.

an agreement and close between them and the little different because of the effect of the connector welding and practical design accuracy.

VI. CONCLUSION

Omega structure planar array is used in the design and analysis of a patch antenna array for miniaturization process. The designed X-band antenna operated in both C and S bands using omega array. Good return loss behaviour is provided by the proposed antenna at different frequencies for Wi-MAX and mobile communication are covered by the proposed antenna. The recommended operating frequency in each band is tabulated in table 3.

TABLE 3. The recommended operating frequency in bands.

	S-Band	C-Band	X-Band
f[GHz]	3.4	5.6	10.1
RL[dB]	-22	-18	-24

TABLE 4. Comparison with related references.

Ref.	RL[dB]	Effi.[%]	Gain [dB]	Dimensions [mm]
[2]	-21	82.5	5.4	8 × 6 ×0.3
[5]	-24	84	5.9	25×15×2
[17]	-23	87.5	5.86	7.5 × 8.8 × 0.25
[22]	-20	99	6.9	15×121×0.4
This Paper	-24	90	8	12.21×12.91×1.27

Table 4 introduces a Comparison with research references, the proposed array introduces G = 8 dB, RL = −24 and 90% efficiency compared with the introduced related search.

ACKNOWLEDGMENT

I would like to express my gratitude to the College of Technological Innovation, Zayed University, Dubai, United Arab Emirates, for their unwavering support and resources that significantly contributed to the successful completion of my research paper.

REFERENCES

[1] A. J. A. Al-Gburi, Z. Zakaria, I. M. Ibrahim, and E. B. A. Halim, "Microstrip patch antenna arrays design for 5G wireless backhaul application at 3.5 GHz," in *Recent Advances in Electrical and Electronic Engineering and Computer Science* (Lecture Notes in Electrical Engineering). Singapore: Springer, 2022, pp. 77–88, doi: 10.1007/978-981-16-9781-4_9.

[2] P. M. Ridoy, A. Saha, K. Y. Fariya, P. Saha, K. M. Elme, and F. Arifin, "Millimeter-wave dual-band slotted antenna for 5G applications," in *Proc. 36th Int. Conf. Adv. Inf. Netw. Appl. (AINA)*, vol. 2. Cham, Switzerland: Springer, Mar. 2022, pp. 19–30.

[3] S.-E. Didi, I. Halkhams, M. Fattah, Y. Balboul, S. Mazer, and M. El Bekkali, "Design of a microstrip antenna patch with a rectangular slot for 5G applications operating at 28 GHz," *TELKOMNIKA (Telecommun. Comput. Electron. Control)*, vol. 20, no. 3, p. 527, Jun. 2022, doi: 10.12928/telkomnika.v20i3.23159.

[4] Y.-F. Tsao, A. Desai, and H.-T. Hsu, "Dual-band and dual-polarization CPW fed MIMO antenna for fifth-generation mobile communications technology at 28 and 38 GHz," *IEEE Access*, vol. 10, pp. 46853–46863, 2022, doi: 10.1109/ACCESS.2022.3171248.

[5] P. Liu, X. W. Zhu, Y. Zhang, X. Wang, C. Yang, and Z. H. Jiang, "Patch antenna loaded with paired shorting pins and H-shaped slot for 28/38 GHz dual-band MIMO applications," *IEEE Access*, vol. 8, pp. 23705–23712, 2020.

[6] Z. Wang, S. Liu, and Y. Dong, "A compact, broadband, monopole-like endfire antenna with reconfigurable patterns for 5G applications," *IEEE Trans. Antennas Propag.*, vol. 70, no. 8, pp. 7199–7204, Aug. 2022, doi: 10.1109/TAP.2022.3165661.

[7] A. Sellier, T. V. Teperik, and A. de Lustrac, "Resonant circuit model for efficient metamaterial absorber," *Opt. Exp.*, vol. 21, no. S6, pp. A997–A1006, 2013, doi: 10.1364/OE.21.00A997.

[8] B. Wang, T. Koschny, and C. M. Soukoulis, "Wide-angle and polarization-independent chiral metamaterial absorber," *Phys. Rev. B, Condens. Matter*, vol. 80, Jul. 2009, Art. no. 033108.

[9] Y. Cheng, H. Yang, Z. Cheng, and B. Xiao, "A planar polarization-insensitive metamaterial absorber," *Photon. Nanostruct.-Fundamentals Appl.*, vol. 9, pp. 8–14, Feb. 2011.

[10] X. Shen, T. J. Cui, J. Zhao, H. F. Ma, W. X. Jiang, and H. Li, "Polarization-independent wide-angle triple-band metamaterial absorber," *Opt. Exp.*, vol. 19, no. 10, pp. 9401–9407, 2011.

[11] D. M. Pozar, *Microwave Engineering*, 3rd ed. Hoboken, NJ, USA: Wiley, 2011.

[12] D. Y. Shchegolkov, A. K. Azad, J. F. O'Hara, and E. I. Simakov, "Perfect subwavelength fishnetlike metamaterial-based film terahertz absorbers," *Phys. Rev. B, Condens. Matter*, vol. 82, Nov. 2010, Art. no. 205117.

[13] L. Huang, D. R. Chowdhury, S. Ramani, M. T. Reiten, S. N. Luo, A. J. Taylor, and H. T. Chen, "Experimental demonstration of terahertz metamaterial absorbers with a broad and flat high absorption band," *Opt. Lett.*, vol. 37, no. 2, pp. 154–156, 2012.

[14] K. B. Alici, A. B. Turhan, C. M. Soukoulis, and E. Ozbay, "Optically thin composite resonant absorber at the near-infrared band: A polarization independent and spectrally broadband configuration," *Opt. Exp.*, vol. 19, no. 15, pp. 14260–14267, 2011.

[15] C. A. Balanis, *Antenna Theory: Analysis and Design*, 3rd ed. Hoboken, NJ, USA: Wiley, 2015.

[16] J. Khan, S. Ullah, U. Ali, F. A. Tahir, I. Peter, and L. Matekovits, "Design of a millimeter-wave MIMO antenna array for 5G communication terminals," *Sensors*, vol. 22, no. 7, p. 2768, Apr. 2022, doi: 10.3390/s22072768.

[17] A. E. Farahat and K. F. Hussein, "Dual-band (28/38 GHz) wideband MIMO antenna for 5G mobile applications," *IEEE Access*, vol. 10, pp. 32213–32223, 2022.

[18] Md. S. Rana and Md. M. Rahman, "Study of microstrip patch antenna for wireless communication system," in *Proc. Int. Conf. Advancement Technol. (ICONAT)*, Jan. 2022, pp. 1–4, doi: 10.1109/ICONAT53423.2022.9726110.

[19] N. H. Biddut, Md. E. Haque, and N. Jahan, "A wide band microstrip patch antenna design using multiple slots at V-band," in *Proc. Int. Mobile Embedded Technol. Conf. (MECON)*, Mar. 2022, pp. 113–116, doi: 10.1109/MECON53876.2022.9751951.

[20] K. Singh, S. Patil, A. Naik, and S. Kadam, "Hexagonal microstrip patch antenna design for UWB application," in *Proc. Int. Conf. Automat., Comput. Commun. (ICACC)*, vol. 44, M. D. Patil and V. A. Vyawahare, Eds. Les Ulis, France, 2022, p. 02004, doi: 10.1051/itmconf/20224402004.

[21] A. Talukder and E. Islam, "Design and simulation study of e shaped slotted microstrip patch antenna by HFSS for 5G applications," in *Proc. IEEE Int. Symp. Antennas Propag. USNC-URSI Radio Sci. Meeting (APS/URSI)*, Dec. 2021, pp. 1909–1910, doi: 10.1109/APS/URSI47566.2021.9704198.

[22] M. S. Rana, S. B. Rana, and M. M. Rahman, "Microstrip patch antennas for various applications: A review," *Indonesian J. Elect. Eng. Comput. Sci.*, vol. 29, no. 3, pp. 1511–1519, Mar. 2023.

[23] A. Jiddney, Z. Mahmud, M. Rahman, L. C. Paul, and M. T. Islam, "A circular shaped microstrip line fed miniaturized patch antenna for 5G applications," in *Proc. 2nd Int. Conf. Sustain. Technol. Ind. 4.0 (STI)*, Dec. 2020, pp. 1–4, doi: 10.1109/STI50764.2020.9350513.

[24] S. K. Ezzuldin, S. O. Hasan, and M. M. Ameen, "Microstrip patch antenna design, simulation and fabrication for 5G applications," *Simul. Model. Pract. Theory*, vol. 116, Apr. 2022, Art. no. 102497, doi: 10.1016/j.simpat.2022.102497.

[25] M. S. Rana and M. M. Rahman Smieee, "Design and analysis of microstrip patch antenna for 5G wireless communication systems," *Bull. Electr. Eng. Informat.*, vol. 11, no. 6, pp. 3329–3337, Dec. 2022, doi: 10.11591/eei.v11i6.3955.

[26] Md. S. Rana and Md. M. Rahman, "Design and operation exploration of a diamond-shape slotted microstrip antenna for digital world high-speed 5G wireless digital technologies," in *Proc. 2nd Asian Conf. Innov. Technol. (ASIANCON)*, Aug. 2022, pp. 1–4, doi: 10.1109/ASIANCON55314.2022.9908769.

AHMED F. MILIGY was born in Cairo, Egypt. He received the M.Sc. and Ph.D. degrees in electrical engineering from Alexandria University, Egypt, in 2008 and 2012, respectively. His research interests include antennas, wave propagation, electromagnetic fields, electromagnetic waves, substrate-integrated waveguides, and nanomaterials. He is the General Co-Chair of the ITC-Egypt 2024 Egypt Conference. He is a reviewer of IEEE conferences.

FATMA TAHER (Senior Member, IEEE) received the Ph.D. degree from the Khalifa University of Science, Technology and Research, United Arab Emirates, in 2014. She is currently the Assistant Dean of the College of Technological Innovation, Zayed University, Dubai, United Arab Emirates. She has published more than 40 papers in international journals and conferences. Her research interests include signal and image processing, pattern recognition, deep learning, machine learning, artificial intelligence, and medical image analysis, especially in detecting cancerous cells, kidney transplants, and autism. In addition to that, her research is watermarking, remote sensing, and satellite images. She served as a member of the steering, organizing, and technical program committees for many international conferences. She has received many distinguished awards, such as the Best Paper Award of the First Prize in the Ph.D. Forum of the 20th IEEE International Conference on Electronics, Circuits, and Systems (ICECS), the Ph.D. Forum, December 2013. She received the UAE Pioneers Award as the first United Arab Emirates to create a computer-aided diagnosis system for early lung cancer detection based on the sputum color image analysis, awarded by H. H. Sheik Mohammed Bin Rashed Al Maktoum, in November 2015. In addition to that, she received the Innovation Award from the 2016 Emirati Women Awards by H. H. Sheik Ahmed Bin Saeed Al Maktoum. She was the Chairman of the Civil Aviation Authority and a Patron of Dubai Quality Group and L'Oréal-UNESCO for Women in Science Middle East Fellowship, in 2017. She is the Vice Chair of the IEEE UAE Section and the Chair of the Education Committee in British Society, United Arab Emirates. She has served on many editorial and reviewing boards for international journals and conferences.

MOHAMED FATHY ABO SREE received the M.Sc. degree from the Arab Academy for Science and Technology, in 2013, and the Ph.D. degree in electrical engineering from Ain Shams University, in 2019. He is currently an Associate Professor with the Department of Electronics and Communication Engineering, Arab Academy for Science Technology and Maritime Transport, Cairo, Egypt. His work notably involves using antennas for cancer detection and ground-penetrating radar systems, highlighting the versatility and significance of his research in both medical diagnostics and subsurface exploration. He has published 100 SCI-indexed research articles and seven SCOPUS-indexed articles, with an H-index of 13 and 521 citations. His research interests include antenna design, microwave technology, biomedical applications, and 5G technologies. He is also a Peer Reviewer of journals, such as IEEE Access and PIER online journal.

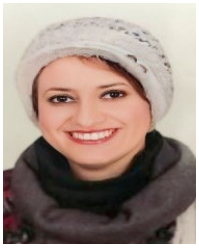

SARA YEHIA ABDEL FATAH was born in Cairo. She received the M.Sc. degree from the Arab Academy for Science and Technology, in 2014. She is currently pursuing the Ph.D. degree with Aswan University. She is currently working as an Assistant Lecturer with the Egyptian Chinese University, Cairo, for eight years.

THAMER ALGHAMDI received the B.Sc. degree from Albaha University, Al Baha, Saudi Arabia, in 2012, the M.Sc. degree from Northumbria University, Newcastle upon Tyne, U.K., in 2016, and the Ph.D. degree from Cardiff University, Cardiff, U.K., in 2023. He was a Power Distribution Engineer with Saudi Electricity Company (SEC), until 2013. From 2016 to 2018, he was a Lecturer Assistant with Albaha University. His main research interests include power systems, power quality, the integration of renewables, and AI applications in electrical engineering.

MOATH ALATHBAH received the Ph.D. degree from Cardiff University, U.K. He is currently an Assistant Professor with King Saud University, Saudi Arabia. His research interests include the development of photoelectronic, integrated electronic active and passive discrete devices, the design, fabrication, and characterization of MMIC, RF and THz components, smart antennas, microstrip antennas, microwave filters, meta-materials, 5G antennas, MIMO antennas miniaturized multiband/wideband antennas, and microwave/millimeter components using micro and nanotechnology.